Catalysis Letters (2019) 149:1075–1086
https://doi.org/10.1007/s10562-019-02675-0

Graphene Oxide Incorporated Strontium Nanoparticles as a Highly Efficient and Green Acid Catalyst for One-Pot Synthesis of Tetramethyl-9-aryl-hexahydroxanthenes and 13-Aryl-5*H*-dibenzo[*b,i*]xanthene-5,7,12,14(13*H*)-tetraones Under Solvent-Free Conditions

Seyyed Rasul Mousavi[1] · Hamid Rashidi Nodeh[2] · Elham Zamiri Afshari[3] · Alireza Foroumadi[1]

Received: 15 November 2018 / Accepted: 13 January 2019 / Published online: 29 January 2019

Abstract

An efficient, inexpensive and recyclable graphene oxide/strontium nanocatalyst was synthesized and applied in a pseudo three-component, one-pot cyclocondensation of aromatic aldehydes and dimedone/lowson to afford the corresponding 3,3,6,6-tetramethyl-9-aryl-3,4,5,6,7,9-hexahydro-1*H*-xanthene-1,8(2*H*)-diones and 13-aryl-5*H*-dibenzo[*b,i*]xanthene-5,7,12,14(13*H*)-tetraones in high yields under solvent-free conditions. To the best of our knowledge, there are no literature reports on applying graphene oxide/strontium as a nanocatalyst for xanthene derivatives synthesis. The key potential benefits of the present method are including high yields, short reaction time, easy workup, recyclability of catalyst and ability to tolerate a variety of functional groups which gives economical as well as ecological rewards. The nanocatalyst easily separated from the reaction mixture easily by applying an external magnet and reused at least six times without noticeable degradation in catalytic activity.

Graphical Abstract

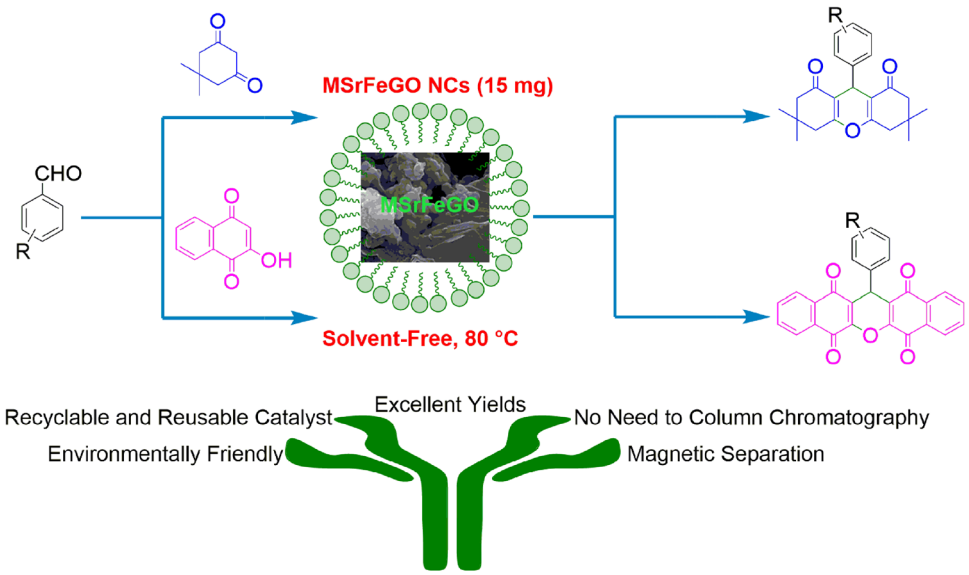

Keywords Xanthene · Lowson · Heterogeneous catalyst · Reusable catalyst · Graphene oxide · One-pot · Magnetic nanocatalyst

Extended author information available on the last page of the article

1 Introduction

In recent years, green chemistry has become a major driving force for organic chemists to develop environmentally benign to a myriad of materials [1]. The development of cleaner technologies is a major subject in green chemistry [2]. Green chemistry concerns the design of environmentally friendly products and chemical processes while minimizing the usage and generation of hazardous substances. Organic solvents are a key factor in environmental pollution and many are carcinogenic and toxic making reactions which do not require the use of organic solvents desirable. Water is an alternative solvent for many chemical reactions, possessing desirable properties such as ready availability, chemical stability, nontoxicity, recyclability and easy handling [3–5]. Moreover, performing of organic reactions under solvent-free conditions is another strategy to avoid the use of hazardous organic solvents [6–8]. On the other hand, one of the arms of green chemistry is the use of heterogeneous green catalysts. In the last decade, the synthesis and application of nanoparticles as heterogeneous catalysts with different shapes and sizes have been developed. The catalytic activity of a heterogeneous catalyst is mainly determined by its morphology and particle size. The catalytic activity can be improved by reducing the particle size to nanometer scale. Because, nanocatalysts exhibit higher activity and selectivity than their corresponding bulk materials. They are expected to be suitable candidates for the design of highly active and selective heterogeneous catalysts for organic synthesis due to their unique physical, surface chemical and catalytic properties and large surface-to-volume ratio [9]. Nevertheless, use of such nanoscales can be increase operating costs but also increase having negative environmental impacts. Since, collection and separation of these nanoparticles from the reaction mixture is almost as difficult as separation using conventional methods [8]. In recent years, a great deal of attention has been paid to the preparation of heterogeneous catalysts by immobilizing magnetic materials on various solid supports [8, 10–13]. Among the many attempts to the various support used for the preparation of heterogeneous catalyst systems, iron oxide magnetic nanoparticles (MNPs) has particular importance because of its availability, high stability and the fact that organic groups can adjoin to its surface with strong connection [14–16]. More importantly, due to the magnetic nature of the catalyst, it could be recovered using an external magnetic field. Also, the isolation of the final product can be possible by a simple decantation. In addition, such catalysts also showed better efficiency, and superior stability when compared to their other supported and unsupported peers. On the other hand, due to having strong magnetic moments of MNPs, they provided various potential applications such as hyper thermal agents, drug delivery, MRI contrast agents and cell sorting [17–22]. Furthermore, extraction of selected cells from biological samples and cell cultures using MNPs has been reported [23].

Supporting organocatalyst on MNPs is a very hopeful research area which widely used for chemical synthesis in organic reactions. Therefore, different organocatalysts were covalently grafted to the MNPs surface and was used in organic transformations [15, 24].

Synthesis of heterocyclic compounds have become an important area of research in organic chemistry [25]. Recently, fused heterocyclic compounds have gained great attention in the field of medicinal chemistry due to their significant contribution in the biological profiling of drugs [26–29]. In this context, of some active carbonyl compounds such as dimedone, thiobarbituric acid, barbituric acid, meldrum's acid and naphthoquinones with various substrates for the synthesis of fused heterocycles have been documented in recent years [27, 29–37]. Among a large variety of fused heterocyclic compounds, xanthene derivatives are valuable synthetic scaffolds for both medicinal and synthetic organic chemists [38–40]. Xanthene derivatives are tricyclic molecules containing pyran scaffold as central a ring fused to aliphatic or aromatic rings on both sides [40]. Xanthenes are an important class of heterocyclic compounds that exhibit significant biological and pharmaceutical properties. These compounds were found to be potent anti-inflammatory [41, 42], antimicrobial [43], antioxidant [44], u-opiat agonist [45], antiproliferative [46], antiviral [47], and antibacterial agents [48]. Xanthene derivatives are also utilized as antagonists for paralyzing action of zoxazolamine and in photodynamic therapy [49]. Moreover, these heterocycles can be widely used in laser technologies, stable dyes, protein labelling fluorophores and fluorescent sensor due to their useful spectroscopic properties [40, 41, 50–52]. Due to their wide range of applications, xanthenes have received a great deal of attention in connection with their synthesis. In this context, a large number of catalytic systems is present in the literature to assemble these interesting scaffolds [1, 39, 42, 47, 53–61]. Most of this recent research though are useful and convenient but, several of these methods suffer from certain drawbacks such as prolonged reactions times, tedious work-up conditions, use of volatile or hazardous organic solvents, employment of large amount of catalyst and harsh reaction conditions. Therefore, due to their manifold applications xanthene derivatives introducing a clean procedure by the use of green and environmentally friendly catalyst with high catalytic activity, moderate temperature, and short reaction time accompanied with excellent yield for the production of this class heterocycles is needed. In view of some previous works, we were thus fascinated by the possibility of applying nanotechnology to the design of a novel, active,

recyclable, and magnetically recoverable organometallic catalyst by using graphene oxide.

Based on the above fundamental understandings and in continuing our ongoing research towards the development of eco-friendly and green multicomponent reactions [28, 37, 62–64], a magnetically recyclable graphene oxide catalyst was assembled using magnetic nanoparticles as the support, and the combined convenient recyclability and excellent activity for the synthesis of tetramethyl-9-aryl-hexahydroxanthenes (**4a–l**) and 13-aryl-5*H*-dibenzo[*b,i*] xanthene-5,7,12,14(13*H*)-tetraones (**5a–n**) in a one-pot, pseudo three-component under solvent-free conditions was demonstrated (Scheme 1). This procedure is very simple, economical and environmentally friendly.

As shown in Scheme 2, the catalyst (MSrGO NCs) was prepared via a simple route and method from inexpensive commercially materials.

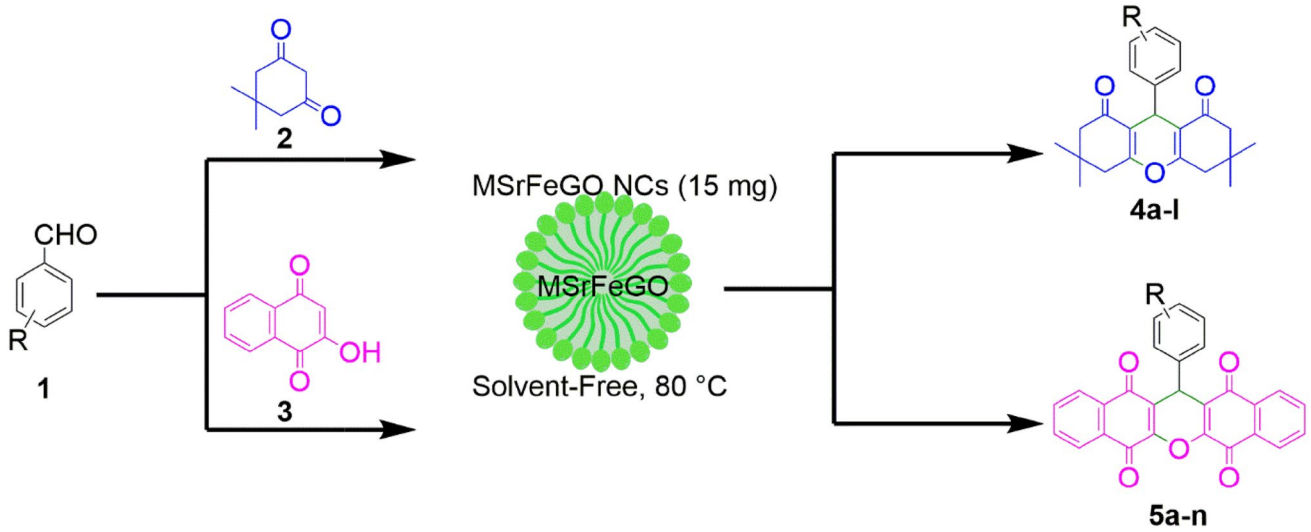

Scheme 1 Synthesis of xanthene derivatives using immobilized graphene oxide on magnetic strontium nanoparticles (MSrGO NCs)

Scheme 2 Graphical route for synthesis of MSrGO nanocatalyst

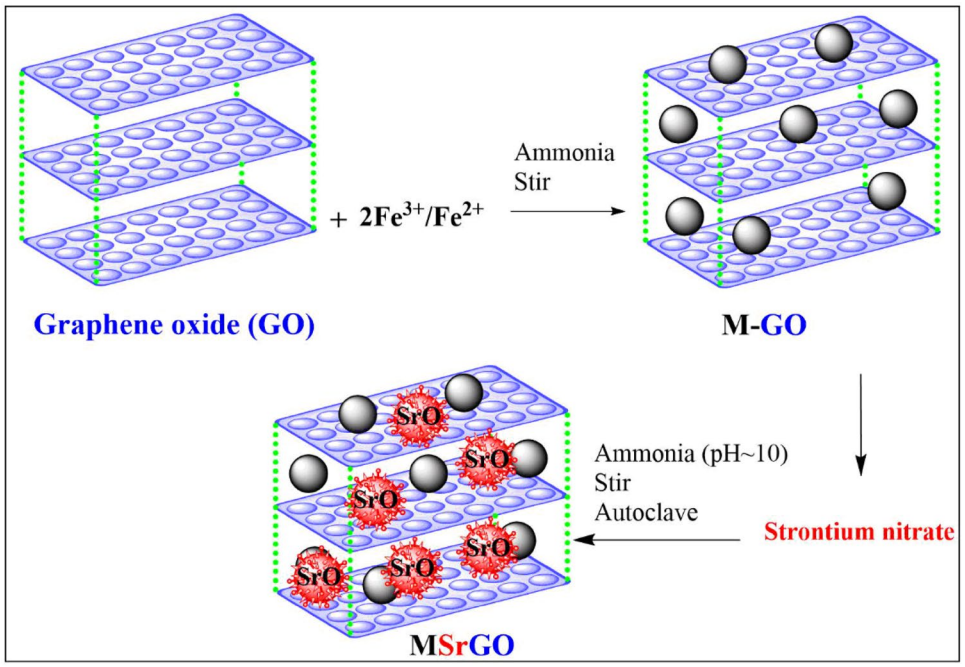

2 Results and Discussion

2.1 Evaluating the Catalytic Activity of the MSrGO NCs

Following our interest to designing and developing a new efficient and environmental friendly heterogeneous catalysts for organic transformations, the MSrGO NCs was initially synthesized [65] according to procedure as shown in Scheme 2. Then, the synthesized catalyst was fully characterized by means of different techniques, such as Fourier transform infrared spectroscopy (FT-IR), small-angle X-ray diffraction (XRD) and field emission scanning electron microscopy (FE-SEM). The results obtained from these techniques confirmed the successful preparation of the new mesoporous catalyst. The present study overcomes some drawbacks of the previous methods, such as longer reaction times, separation of catalyst, hazardous solvents and expensive catalyst required for the green, one-pot, pseudo three-component synthesis of xanthene derivatives via the condensation reaction between aromatic aldehydes and dimedone/lawsone. The reaction conditions have been optimized by the reaction of benzaldehyde **1** (1 mmol), and dimedone **2** (2 mmol) as model reaction to result in, 3,3,6,6-tetramethyl-9-phenyl-3,4,5,6,7,9-hexahydro-1*H*-xanthene-1,8(2*H*)-dione **4a**. The model reaction was optimized in terms of various parameters such as effect of solvent, catalyst amount, and influence of temperature. A summary of the optimization experiments is provided in Table 1. At the beginning, two uncatalyzed reactions were tested under solvent-free conditions (One at room temperature and another at 80 °C) but no significant yield was obtained even after 24 h (Table 1, entries 1 and 2). Then, the test reaction was studied in the presence of 5 mg under solvent-free conditions, as well as with different solvents such as EtOH, MeOH, EtOAc, CH_2Cl_2, CH_3CN and H_2O to assess the solvent effect on the reaction rate at 80 °C (Table 1, entries 3–9). It was observed that the reaction proceeds moderately in the presence of various solvents, but when the reaction was carried out under solvent-free reaction conditions, maximum yield (75%) was obtained at

Table 1 Optimization of conditions for the synthesis of **4a**

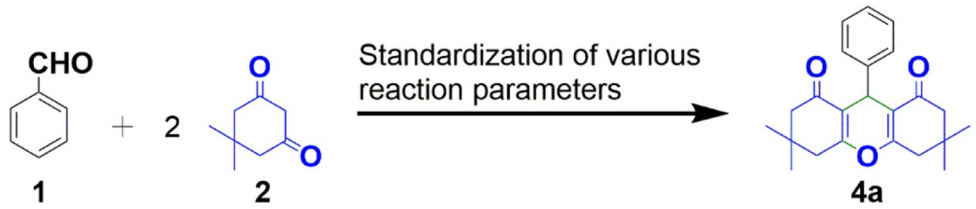

Entry	Catalyst (mg)	Solvent	Temperature (°C)	Time (h)	Yield (%)[a]
1	–	–	RT	24	–
2	–	–	80	24	–
3	5	EtOH	80	5	65
4	5	MeOH	80	5	65
5	5	EtOAc	80	5	56
6	5	CH_2Cl_2	80	5	47
7	5	MeCN	80	5	66
8	5	H_2O	80	5	45
9	5	–	80	5	75
10	10	–	80	3	85
11	**15**	**–**	**80**	**2.5**	**92**
12	20	–	80	2.5	92
13	25	–	80	3	90
14	30	–	80	3	91
15	15	–	40	8	53
16	15	–	60	8	68
17	15	–	100	3	90
18	15	–	110	2.5	91

[a]Yield refers to the pure isolated product

80 °C (Table 1, entry 8). Following choice of solvent-free conditions, the effect of the catalyst loading on yields of the reaction was assessed (Table 1, entries 9–14). Various sets of reactions were carried with different catalyst concentrations ranging from 5 to 30 mg at 80 °C. It was observed that with increasing the catalyst concentration, yield of the product increases. Maximum yield (92%) was obtained when 15 mg of catalyst was used (Table 1, entry 11). Further increase in the catalyst loading (25 and 30 mg) had no significant effect on the yield of the reaction (Table 1, entries 13 and 14).

During the optimization of the reaction conditions, the effect of temperature on the pilot reaction was also evaluated at 40, 60, 80, 100 and 110 °C to test their efficiency under solvent-free conditions (Table 1, entries 11 and 15–18). It was observed that the yield of the product is maximum at 80 °C (Table 1, entry 11). Hence, 80 °C was chosen as optimum temperature for the reaction. Therefore, as shown in Table 1, using 15 mg MSrGO NCs under solvent-free and 80 °C gave the highest yield of 3,3,6,6-tetramethyl-9-phenyl-3,4,5,6,7,9-hexahydro-1*H*-xanthene-1,8(2*H*)-dione **4a** in the shortest time.

With these encouraging results in hand, the generality of this reaction was examined using various aromatic aldehydes containing electron-donating as well as electron-withdrawing groups. All the substrate variants reacted well and afforded higher yields of 3,3,6,6-tetramethyl-9-aryl-3,4,5,6,7,9-hexahydro-1*H*-xanthene-1,8(2*H*)-diones in shorter reaction times without formation of any byproducts (Table 2). The investigation of results shows that the nature of substitutions on aromatic aldehydes has no significant effect on the reaction time and yields under the above optimal conditions (Table 2, entries 2–12).

The scope and generality of the present protocol were also extended by condensation of two equivalents of 2-hydroxynaphthalene-1,4-dione and one equivalent of aryl aldehydes containing the electron-withdrawing or electron-donating substituents (Scheme 1). The reaction progressed smoothly with both electron-withdrawing and electron-donating aromatic aldehydes to get higher yields of the corresponding 13-aryl-5*H*-dibenzo[*b,i*]xanthene-5,7,12,14(13*H*)-tetraones in shorter reaction time (Table 3). The position of the substituent on the phenyl ring of aryl aldehydes showed no significant effect on the yield and time of the reaction.

In order to assess the efficiency of this methodology, the obtained result from the reaction of 4-methyl benzaldehyde with 2-hydroxynaphthalene-1,4-dione for the synthesis of 13-(*p*-tolyl)-12*H*-dibenzo[*b,i*]xanthene-5,7,12,14(13*H*)-tetraone (**5b**) by this procedure has been compared with those of the previously reported in the literature. As shown in Table 4, the use of MSrGO NCs leads to an improved protocol in terms of compatibility with environment, reaction time, yield of the product, and amount of the catalyst when compared with other catalysts.

The end in order to make the procedure economically and environmentally more viable, we also carried out a

Table 2 Synthesis of 3,3,6,6-tetramethyl-9-aryl-3,4,5,6,7,9-hexahydro-1*H*-xanthene-1,8(2*H*)-diones by SrFeGO nanocomposite

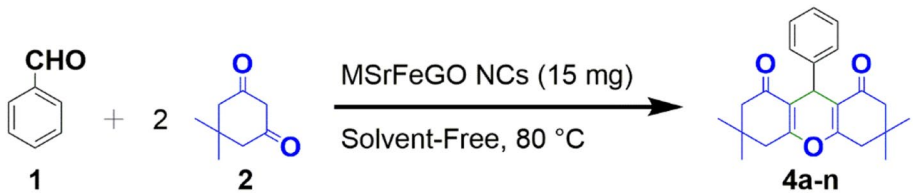

Entry	R	Product	Time (h)	Yield (%)[a]	M.p (°C)	M.p (°C) [References]
1	H	**4a**	2.5	92	199–200	198–200 [1]
2	4-CH_3	**4b**	3	89	211–213	212–214 [66]
3	2-Br	**4c**	1	97	227–229	226–229 [60]
4	2-Cl	**4d**	1	90	226–228	226–228 [67]
5	4-Cl	**4e**	1	92	232–234	230–232 [68]
6	2-NO_2	**4f**	0.9	91	248–250	248–249 [69]
7	3-NO_2	**4g**	4	93	170–172	171–173 [66]
8	4-NO_2	**4h**	1.5	96	220–222	221–223 [67]
9	4-$N(CH_3)_2$	**4i**	5	80	220–222	221–223 [66]
10	4-OCH_3	**4j**	1.5	94	240–242	239–241 [70]
11	3,4-$(OCH_3)_2$	**4k**	1.5	93	181–183	182–184 [1]
12	3,4,5-$(OCH_3)_3$	**4l**	0.8	90	190–192	192–194 [71]

[a]Isolated yield

Table 3 Construction of 13-aryl-5*H*-dibenzo[*b,i*]xanthene-5,7,12,14(13*H*)-tetraone derivatives in the presence of MSrGO NCs

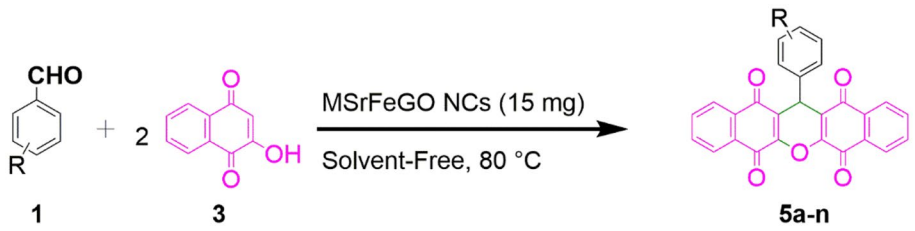

Entry	R	Product	Time (h)	Yield (%)[a]	M.p (°C)	M.p (°C) [Ref]
1	H	**5a**	2.5	90	304–306	305–307 [72]
2	4-CH_3	**5b**	2	92	303–305	304–307 [73]
3	2-Br	**5c**	1	96	282–284	283–285 [72]
4	4-Br	**5d**	0.8	94	> 310	> 320 [74]
5	2-OCH_3	**5e**	2.5	89	262–264	263–264 [55]
6	4-OCH_3	**5f**	2	92	> 310	320–322 [54]
7	2-NO_2	**5g**	2	91	272–274	273–277 [55]
8	3-NO_2	**5h**	1.75	95	> 310	340–342 [58]
9	4-NO_2	**5k**	1.5	93	> 310	> 330 [55]
10	2-Cl	**5l**	1.75	90	306–308	304–306 [54]
11	3-Cl	**5m**	2	88	279–281	280–282 [55]
13	4-Cl	**5n**	1.75	89	> 310	330–332 [58]

[a]Isolated yield

Table 4 Comparative study of the present methodology with others reported in the literature for the synthesis of compound **5b**

Entry	Catalyst	Reaction conditions	Time (min)	Yield (%)[a]	[References]
1	ChCl/itaconic acid	80 °C	120	91	[55]
2	[Msim]Cl	Solvent-free, 80 °C	7	88	[53]
3	[Hmim]HSO_4^-	Solvent-free, 80 °C	7	90	[53]
4	[Et_3N–SO_3H]Cl	Solvent-free, 80 °C	8	90	[53]
5	[Et_3NH][HSO_4]	Solvent-Free, 80 °C	9	89	[53]
6	H_2SO_4	EtOH, reflux	150	91	[54]
7	bmim[HSO_4]	80 °C	90	84	[54]
8	*p*-TSA	Solvent-free/80 °C	420	70	[58]
9	*p*-TSA	Solvent-free/100 °C	240	78	[73]
10	TMGT/TFA	75 °C	60–132	84	[47]
11	MSrGO NCs	Solvent-free/80 °C	120	92	This work

[a]Isolated yield

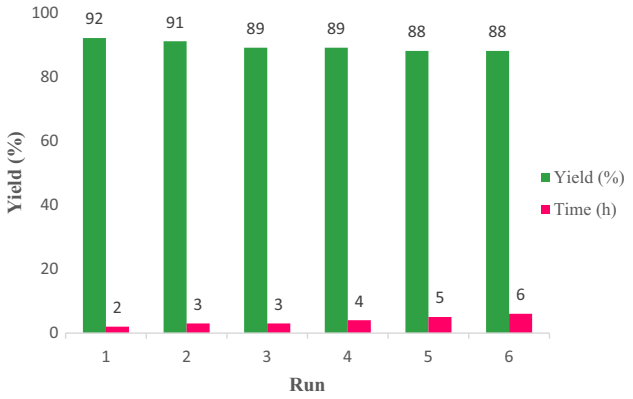

Fig. 1 Recyclability studies of MSrGO NCs in the synthesis of the product **5b**

reaction to inspect reusability of MSrGO NCs. As soon as the reaction was complete, the catalyst was separated easily by an external magnetic field and washed with ethanol for several times and dried. The catalytic activity of recycled MSrGO NCs was tested under optimal reaction conditions for the synthesis of 13-(*p*-tolyl)-12*H*-dibenzo[*b,i*] xanthene-5,7,12,14(13*H*)-tetraone (**5b**), and it was found that recycled MSrGO NCs furnished the product in good to high yield. Likewise, this catalyst can be reused in six more consecutive runs (Fig. 1) with only a modest loss in catalytic activity.

3 Experimental

3.1 General

All solvents, chemicals and reagents were research grade and purchased from Merck, Fluka and Sigma Aldrich chemical companies and used without further purification. All reactions and the purity of the products were monitored by thin-layer chromatography (TLC) on F254 aluminium plates coated with silica gel (Merck) using petroleum ether/ethyl acetate (8:2) as the eluent solvent. Melting points were recorded on an Electrothermal 9100 apparatus. Ultraviolet light was used for spots identification during the reaction process. Functional groups of the products were characterized using FT-IR spectroscopy and spectra were recorded in the range of 400–4000 cm^{-1} by a Bruker Equinox 55 FT-IR spectrometer (Bremen, Germany). Bruker NMR-500 MHZ spectrometer applied for recording of ^{1}H NMR spectra. Elemental composition and morphology of the magnetic nanocatalyst were studied using TESCAN MIRA3 FE-SEM equipped with EDX analyzed (Prague, Czech Republic).

3.2 Preparation of MSrGO Nanocomposite

Magnetic nanoparticles doped graphene oxide (M–GO) was prepared by dissolving of proper amount of $FeCl_3.6H_2O$ (200 mg), $FeCl_2.4H_2O$ (400 mg) and grapheme oxide (500 mg) in distilled water (50 mL). To get homogenize solution the mixture was sonicated for 30 min then ammonia solution (2 mL, 25%) was added drop-vise and stirred vigorously for 5 h. The dark black product was collected by assistance of external magnet and washed with excess distilled water and oved dried at 80 °C for 24 h. For further experiment, M–GO nanocomposite was modified with strontium nanoparticles to get MSrGO nanocatalyst. Consequently, strontium nitrate solution (0.1 M) was prepared in distilled water then 500 mg of M–GO powder was added and sonicated for 30 min. Then, reaction temperature was set at 45 °C followed by addition of 1 M ammonia solution (dropwise) to set solution pH at 9–10 under vigorous stirring for 1 h. finally, solution was transferred to autoclave and kept for 24 h at 120 °C. Product was washed with excess distilled water and oven dried at 80 °C for 24 h before using.

3.3 Catalyst Characterization

3.3.1 FT-IR Spectroscopy

FT-IR spectroscopy (Fig. 2) is represent the characteristics functional groups of as prepared M-GO and MSrGO nanocatalyst. The M–GO spectrum provided several IR bands at 3431, 1636, 1378, 1097 and 592 cm^{-1} that are corresponding to O–H stretching, C=O, C–C/C–O (epoxy), C–OH and F–O, respectively. As can be seen, after modification of M–GO with strontium nanoparticles some IR bands are appeared and disappeared in MSrGO spectrum. Hence, the

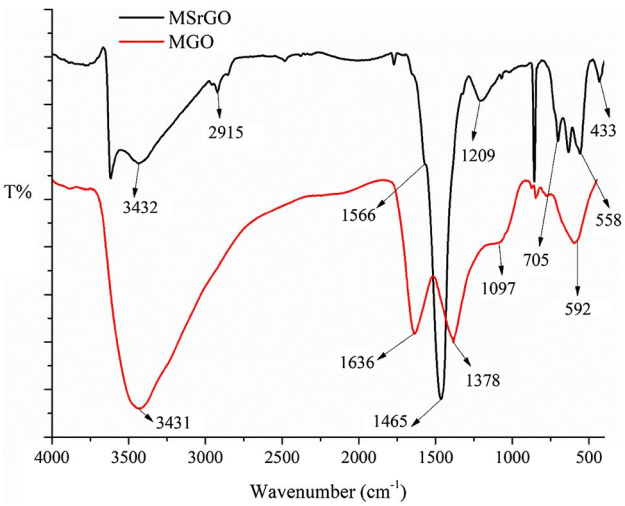

Fig. 2 FT-IR spectrum of the synthesized MSrGO NCs

IR bands for MSrGO are as following 3620, 3434, 2921, 1769, 1620, 1450, 1208, 690, 556 and 460 cm^{-1}. The peaks at 3620 cm^{-1} and 1620 cm^{-1} are enhancing the O–H stretching and bending. The characteristics bands at 2921, 1769, 1450, 1208 are corresponding to C–H, C=O, C=C/C–C and C–OH, respectively. The presence of strontium nanoparticles on the nanocatalyst can be claimed with two peaks at 690 cm^{-1} and 460 cm^{-1} that attribute the Sr–O band. Finally, the IR signal at 556 cm^{-1} confirm the presence of magnetic iron oxide substance (Fe–O) on the nanocatalyst.

3.3.2 FESEM Microscopy

Surface micrograph of the MSrGO nanocatalyst was studied with FESEM microscopy technique. Hence, the FESEM micrograph (Fig. 3) shows the sheet like layers with some dispersed nanoparticles. Probably the flake sheets are corresponding to grapheme oxide layers and nanoparticles are corresponding to the strontium and iron oxide nanoparticles. It is noteworthy that the nanoparticles are well dispersed on the surface of graphene sheets. The particle size was monitored with *Image J* software for 60 particles and average size obtained was 71.9 nm. These are provided the successful synthesis of the nanocatalyst. The expected elements on the nanoctalyste were analyzed with energy-dispersive X-ray spectroscopy technique and C, O, Fe and Sr, elements were as 32, 23, 29 and 14%, respectively.

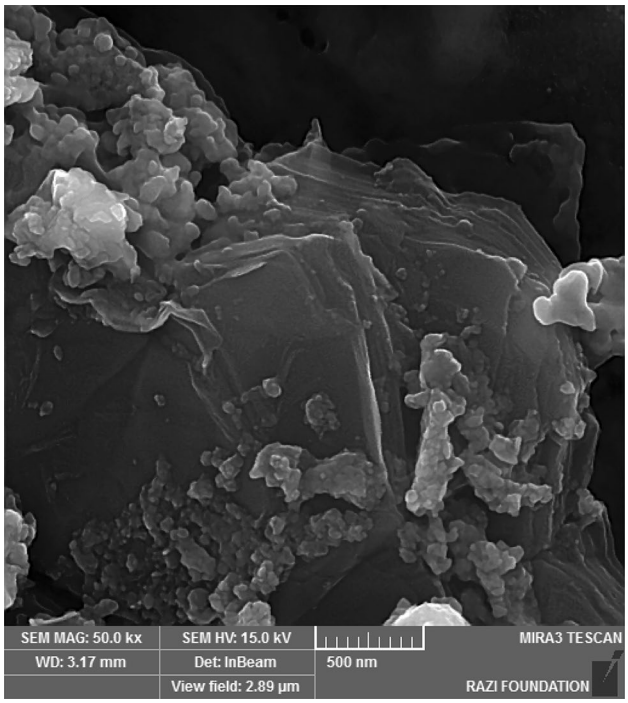

Fig. 3 SEM image of the synthesized MSrGO NCs

3.3.3 XRD Diffractometer

The crystalline structure of MSrGO NCs was investigate through small-angle XRD analysis. The XRD signals for both magnetic Fe_3O_4 nanoparticle and MSrGO NCs are depicts in Fig. 4. Both patterns are showing the various XRD signals at different angle (2 theta) that directly reflect the crystalline structure of bot materials. The characteristics signals for magnetic Fe_3O_4 nanoparticles are approximately observed at 25°, 30.2°, 35.4°, 43.1°, 53.6°, 57° and 63° and for strontium are approximately at 28°, 33°, 38, 42°, 48, 50, 52, 55°, 67°. The sharp signal at 18° (002) is reflecting the graphene oxide skeleton. Thus, it can be claim that the MSrGO NCs is possessing crystalline structure that it is suitable for catalyst purposes.

3.4 General Experimental Procedure for Synthesis of Xanthene Derivatives

In a topical procedure, a mixture of substituted benzaldehydes (1 mmol), and dimedone (2 mmol)/2-hydroxynaphthalene-1,4-dione (2 mmol) was stirred at 80 °C utilizing MSrGO NCs (15 mg) in solvent-free condition for the time period as indicated in Tables 2 and 3 until the reaction was complete. Upon completion of the reaction, monitored by TLC, the mixture was cooled to room temperature. With completing the reaction, 5 mL ethanol was poured and the magnetic nanocomposite was removed by an external magnet, then the precipitated products were separated by filtration and recrystallized from ethanol to furnish pure xanthene derivatives. All products have been reported previously. The pure products were characterized by conventional spectroscopic methods. Physical and spectral data for the selected compounds **4a, 4e, 4k, 5c, 5f–h, 5l** and **5n** are shown below:

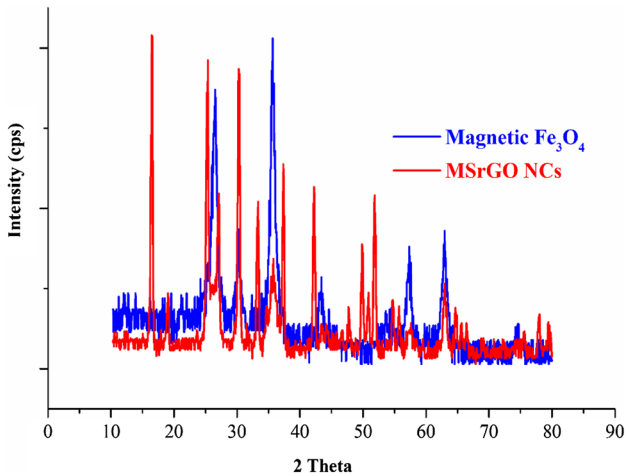

Fig. 4 XRD pattern for MSrGO NCs

3.4.1 3,3,6,6-Tetramethyl-9-phenyl-3,4,5,6,7,9-hexahydro-1*H*-xanthene-1,8(2*H*)-dione (**4a**)

White solid, yield: (92%); m.p. 199–200 °C. ^{1}H NMR (500 MHz, DMSO): 1.04 (s, 12H, $4CH_3$), 2.09 (s, 4H, $2CH_2$), 2.20 (s, 4H, $2CH_2$), 5.94 (s, 1H, CH), 7.05–7.10 (m, 5H, Ar–H).

3.4.2 9-(4-Chlorophenyl)-3,3,6,6-tetramethyl-3,4,5,6,7,9-hexahydro-1*H*-xanthene-1,8(2*H*)-dione (**4e**)

White solid, yield: (92%); m.p. 232–234 °C. ^{1}H NMR (500 MHz, DMSO): 0.98 (s, 6H, $2CH_3$), 1.02 (s, 6H, $2CH_3$), 2.08 (s, 4H, $2CH_2$), 2.24 (s, 4H, $2CH_2$), 4.49 (s, 1H, CH), 7.17 (d, $J=7.5$ Hz, 2H, Ar-H), 7.26 (d, $J=7.5$ Hz, 2H, Ar–H).

3.4.3 9-(3,4-Dimethoxyphenyl)-3,3,6,6-tetramethyl-3,4,5,6,7,9-hexahydro-1*H*-xanthene-1,8(2*H*)-dione (**4k**)

White solid, yield: (93%); m.p. 181–183 °C. ^{1}H NMR (500 MHz, DMSO): 0.75 (s, 6H, $2CH_3$), 0.89 (s, 6H, $2CH_3$), 2.06 (s, 4H, $2CH_2$), 2.19 (s, 4H, $2CH_2$), 3.35 (s, 3H, OCH_3), 3.69 (s,3H, OCH_3), 4.98 (s, 1H, CH), 7.67 (s, 1H, Ar-H), 7.40 (d, $J=7.8$ Hz, 2H, Ar–H).

3.4.4 13-(2-Bromophenyl)-12*H*-dibenzo[*b,i*]xanthene-5,7,12,14(13*H*)-tetraone (**5c**)

Yellow solid, yield: (96%); m.p. 282–284 °C. ^{1}H NMR (500 MHz, DMSO): 6.85 (s, 1H, CH), 7.36 (t, $J=7.3$ Hz, 1H, Ar–H), 7.42 (d, $J=7.8$ Hz, 1H, Ar–H), 7.49 (t, $J=7.5$ Hz, 1H, Ar–H), 7.58 (d, $J=7.8$ Hz, 1H, Ar–H), 7.68 (t, $J=7.4$ Hz, 2H, Ar–H), 7.77 (t, $J=7.4$ Hz, 2H, Ar–H), 7.88 (d, $J=7.4$ Hz, 2H, Ar–H), 7.95 (d, $J=7.5$ Hz, 2H, Ar–H).

3.4.5 13-(4-Methoxyphenyl)-12*H*-dibenzo[*b,i*]xanthene-5,7,12,14(13*H*)-tetraone (**5f**)

Red solid, yield: (92%); m.p. >310 °C. ^{1}H NMR (500 MHz, DMSO): 3.69 (s, 3H, OCH_3), 5.94 (s, 1H, CH), 6.75 (d, $J=7.5$ Hz, 2H, Ar–H), 7.13 (d, $J=7.0$ Hz, 2H, Ar–H), 7.78 (d, $J=7.0$ Hz, 1H, Ar–H), 7.81 (d, $J=7.0$ Hz, 2H, Ar–H), 7.91 (d, $J=6.5$ Hz, 2H, Ar–H), 7.97 (d, $J=6.5$ Hz, 2H, Ar–H).

3.4.6 13-(2-Nitrophenyl)-12*H*-dibenzo[*b,i*]xanthene-5,7,12,14(13*H*)-tetraone (**5g**)

Yellow solid, yield: (91%); m.p. 272–274 °C. ^{1}H NMR (500 MHz, DMSO): 6.63 (s, 1H, CH), 7.37 (t, $J=7.3$ Hz, 1H, Ar–H), 7.42 (d, $J=7.8$ Hz, 1H, Ar–H), 7.49 (t, $J=7.4$ Hz, 1H, Ar–H), 7.59 (d, $J=7.8$ Hz, 1H, Ar–H), 7.68 (t, $J=7.3$ Hz, 2H, Ar–H), 7.77 (t, $J=7.3$ Hz, 2H, Ar–H), 7.88 (d, $J=7.5$ Hz, 2H, Ar–H), 7.95 (d, $J=7.5$ Hz, 2H, Ar–H).

3.4.7 13-(3-Nitrophenyl)-12*H*-dibenzo[*b,i*]xanthene-5,7,12,14(13*H*)-tetraone (**5h**)

Orange solid, yield: (95%); m.p. >310 °C. ^{1}H NMR (500 MHz, DMSO): 6.65 (s, 1H, CH), 7.49 (t, $J=7.9$ Hz, 1H, Ar–H), 7.65 (d, $J=7.6$ Hz, 1H, Ar–H), 7.71 (t, $J=7.4$ Hz, 2H, Ar–H), 7.78 (t, $J=7.4$ Hz, 2H, Ar–H), 7.91 (t, $J=7.2$ Hz, 3H, Ar–H), 7.97 (d, $J=7.9$ Hz, 3H, Ar–H).

3.4.8 13-(2-Chlorophenyl)-12*H*-dibenzo[*b,i*]xanthene-5,7,12,14(13*H*)-tetraone (**5l**)

Dark green solid, yield: (90%); m.p. 306–308 °C. ^{1}H NMR (500 MHz, DMSO): 6.46 (s, 1H, CH), 7.42–7.45 (m, 1H, Ar–H), 7.54 (d, $J=4.0$ Hz, 2H, Ar–H), 7.78 (t, $J=7.4$ Hz, 2H, Ar–H), 7.83 (t, $J=7.6$ Hz, 2H, Ar–H), 7.84 (t, $J=4.7$ Hz, 1H, Ar–H), 7.93 (d, $J=7.5$ Hz, 2H, Ar–H), 7.98 (d, $J=7.5$ Hz, 2H, Ar–H),.

3.4.9 13-(4-Chlorophenyl)-12*H*-dibenzo[*b,i*]xanthene-5,7,12,14(13*H*)-tetraone (**5n**)

Yellow solid, yield: (89%); m.p. >310 °C. ^{1}H NMR (500 MHz, DMSO): 6.47 (s, 1H, CH), 7.04 (d, $J=7.5$ Hz, 2H, Ar–H), 7.15 (d, $J=7.5$ Hz, 2H, Ar–H), 7.63 (t, $J=7.5$ Hz, 2H, Ar–H), 7.70 (t, $J=7.5$ Hz, 2H, Ar–H), 8.02 (d, $J=7.5$ Hz, 2H, Ar–H), 8.12 (d, $J=7.5$ Hz, 2H, Ar–H).

4 Conclusion

In conclusion, we have developed a proficient, magnetic graphite oxide-based (MSrGO NCs) catalyzed procedure for the synthesis of xanthene derivatives under solvent-free reaction conditions. Easy handling of the catalyst, high reusability, shorter reaction time, and solvent-free reaction conditions are the plus points of this methodology which makes the process ecofriendly, sustainable, and green. Moreover, high tolerance of this procedure toward various functional groups, easy work up, exceptionally high yields of desired products, and easy separation of catalyst by an external magnetic field are added advantages for its application to academic and industrial purposes. We believe this will present a better and more practical alternative to the existing methodologies and will find useful application in organic synthesis.

Acknowledgements Authors would like to thank Iran's National Elites Foundation for the financial support and Tehran University of Medical Sciences for facilities and financial support.

Compliance with Ethical Standards

Conflict of interest On behalf of all authors, the corresponding author states that there is no conflict of interest.

References

1. Maleki B, Akbarzadeh E, Babaee S (2015) New basic ionic liquid from ethan-1,2-diyl bis (hydrogen sulfate) and DBU (1,8-diazobicyclo[5.4.0]undec-7-ene) as an efficient catalyst for one-pot synthesis of xanthene derivatives. Dye Pigment 123:222–234
2. Zhang W, Cue BW (2018) Green techniques for organic synthesis and medicinal chemistry. John Wiley & Sons, New Jersey
3. DeSimone JM (2002) Practical approaches to green solvents. Science 297:799–803
4. Kommi DN, Kumar D, Chakraborti AK (2013) "All water chemistry" for a concise total synthesis of the novel class anti-anginal drug (RS),(R), and (S)-ranolazine. Green Chem 15:756–767
5. Otto S, Engberts JBFN (2000) Diels_Alder reactions in water. Pure Appl Chem 72:1365–1372
6. Kolvari E, Koukabi N, Hosseini MM, Vahidian M, Ghobadi E (2016) Nano-ZrO_2 sulfuric acid: a heterogeneous solid acid nano catalyst for Biginelli reaction under solvent free conditions. RSC Adv 6:7419–7425
7. Maleki A, Jafari AA, Yousefi S (2017) $MgFe_2O_4$/cellulose/SO_3H nanocomposite: a new biopolymer-based nanocatalyst for one-pot multicomponent syntheses of polysubstituted tetrahydropyridines and dihydropyrimidinones. J Iran Chem Soc 14:1801–1813
8. Tabrizian E, Amoozadeh A (2016) A new type of SO_3H-functionalized magnetic-titania as a robust magnetically-recoverable solid acid nanocatalyst for multi-component reactions. RSC Adv 6:96606–96615
9. Mardani HR (2017) Cu/Ni)–Al layered double hydroxides@ Fe_3O_4 as efficient magnetic nanocomposite photocatalyst for visible-light degradation of methylene blue. Res Chem Intermed 43:5795–5810
10. Tabrizian E, Amoozadeh A, Rahmani S (2016) Sulfamic acid-functionalized nano-titanium dioxide as an efficient, mild and highly recyclable solid acid nanocatalyst for chemoselective oxidation of sulfides and thiols. RSC Adv 6:21854–21864
11. Ngnie G, Dedzo GK, Detellier C (2016) Synthesis and catalytic application of palladium nanoparticles supported on kaolinite-based nanohybrid materials. Dalt Trans 45:9065–9072
12. Hajjami M, Tahmasbi B (2015) Synthesis and characterization of glucosulfonic acid supported on Fe_3O_4 nanoparticles as a novel and magnetically recoverable nanocatalyst and its application in the synthesis of polyhydroquinoline and 2,3-dihydroquinazolin-4(1*H*)-one derivatives. RSC Adv 5:59194–59203
13. Bhanja P, Bhaumik A (2016) Porous nanomaterials as green catalyst for the conversion of biomass to bioenergy. Fuel 185:432–441
14. Dalpozzo R (2015) Magnetic nanoparticle supports for asymmetric catalysts. Green Chem 17:3671–3686
15. Panahi F, Dangolani SK, Khalafi-Nezhad A (2016) Synthesis of a novel magnetic reusable organocatalyst based on 4-dialkylaminopyridines for acyl transformations. ChemistrySelect 1:3541–3547
16. Wang D, Astruc D (2014) Fast-growing field of magnetically recyclable nanocatalysts. Chem Rev 114:6949–6985
17. Berry CC, Curtis ASG (2003) Functionalisation of magnetic nanoparticles for applications in biomedicine. J Phys D 36:R198–R206
18. Nasongkla N, Bey E, Ren J, Ai H, Khemtong C, Guthi JS, Chin S-F, Sherry AD, Boothman DA, Gao J (2006) Multifunctional polymeric micelles as cancer-targeted, MRI-ultrasensitive drug delivery systems. Nano Lett 6:2427–2430
19. Arruebo M, Fernández-Pacheco R, Ibarra MR, Santamaría J (2007) Magnetic nanoparticles for drug delivery. Nano Today 2:22–32
20. Dobson J (2006) Magnetic nanoparticles for drug delivery. Drug Dev Res 67:55–60
21. Lewin M, Carlesso N, Tung C-H, Tang X-W, Cory D, Scadden DT, Weissleder R (2000) Tat peptide-derivatized magnetic nanoparticles allow in vivo tracking and recovery of progenitor cells. Nat Biotechnol 18:410–414
22. Govan J, Gun'ko YK (2014) Recent advances in the application of magnetic nanoparticles as a support for homogeneous catalysts. Nanomaterials 4:222–241
23. Wang X, Starz-Gaiano M, Bridges T, Montell D (2008) Purification of specific cell populations from Drosophila tissues by magnetic bead sorting, for use in gene expression profiling. Protoc Exch. https://doi.org/10.1038/nprot.2008.28
24. Mrówczyński R, Nan A, Liebscher J (2014) Magnetic nanoparticle-supported organocatalysts—an efficient way of recycling and reuse. RSC Adv 4:5927–5952
25. Safaei-Ghomi J, Shahbazi-Alavi H, Teymuri R (2016) Nano ZrP_2O_7 catalyzed multicomponent reaction for an easy access of 4*H*-pyrans and 1,4-dihydropyridines. Polycycl Aromat Compd 36:834–847
26. Ghashang M, Kargar M, Shafiee MRM, Mansoor SS, Fazlinia A, Esfandiari H (2015) CuO nano-structures prepared in rosmarinus officinalis leaves extract medium: efficient catalysts for the aqueous media preparation of dihydropyrano [3,2-*c*] chromene derivatives. Recent Pat Nanotechnol 9:204–211
27. Mousavi MR, Maghsoodlou MT (2015) Nano-SiO_2: a green, efficient, and reusable heterogeneous catalyst for the synthesis of quinazolinone derivatives. J Iran Chem Soc 12:743–749
28. Mousavi MR, Maghsoodlou MT, Hazeri N, Habibi-Khorassani SM (2015) A simple, economical, and environmentally benign protocol for the synthesis of [1,2,4] triazolo[5,1-*b*]quinazolin-8(4*H*)-one and hexahydro[4,5]benzimidazolo[2,1-*b*]quinazolinone derivatives. J Iran Chem Soc 12:1419–1424
29. Maleki A, Ravaghi P, Aghaei M, Movahed H (2017) A novel magnetically recyclable silver-loaded cellulose-based bionanocomposite catalyst for green synthesis of tetrazolo[1,5-*a*] pyrimidines. Res Chem Intermed 43:5485–5494
30. Safaei-Ghomi J, Sadeghzadeh R, Shahbazi-Alavi H (2016) A pseudo six-component process for the synthesis of tetrahydrodipyrazolo pyridines using an ionic liquid immobilized on a $FeNi_3$ nanocatalyst. RSC Adv 6:33676–33685
31. Safaei-Ghomi J, Shahbazi-Alavi H, Ziarati A (2017) A comparative screening of the catalytic activity of nanocrystalline $M^{II}Zr_4(PO_4)_6$ ceramics in the one-pot synthesis of 1, 6-diamino-4-aryl-2-oxo-1,2-dihydropyridine-3,5-dicarbonitrile derivatives. Res Chem Intermed 43:91–101
32. Mousavi MR, Aboonajmi J, Taher Maghsoodlou M, Hazeri N, Habibi-Khorassani SM, Safarzaei M (2013) $La(NO_3)_3.6H_2O$ catalyzed one-pot highly diastereoselective synthesis of functionalized piperidines. Lett Org Chem 10:171–177
33. Ferreira SB, de Carvalho da Silva F, Bezerra FAFM, Lourenço MCS, Kaiser CR, Pinto AC, Ferreira VF (2010) Synthesis of α-and β-pyran naphthoquinones as a new class of antitubercular agents. Arch Pharm (Weinheim) 343:81–90
34. Maleki B, Babaee S, Tayebee R (2015) $Zn(L\text{-proline})_2$ as a powerful and reusable organometallic catalyst for the very fast synthesis of 2-amino-4*H*-benzo[*g*]chromene derivatives under solvent-free conditions. Appl Organomet Chem 29:408–411

35. Shirini F, Langarudi MSN, Daneshvar N, Mashhadinezhad M, Nabinia N (2017) Preparation of a new DABCO-based ionic liquid and investigation on its application in the synthesis of benzimidazoquinazolinone and pyrimido[4,5-*b*]-quinoline derivatives. J Mol Liq 243:302–312
36. Nikoofar K, Khademi Z (2017) Barbituric acids in organic transformations, an outlook to the reaction media. Mini Rev Org Chem 14:143–173
37. Hazeri N, Maghsoodlou MT, Mousavi MR, Aboonajmi J, Safarzaei M (2015) Potassium sodium tartrate as a versatile and efficient catalyst for the one-pot synthesis of pyran annulated heterocyclic compounds in aqueous media. Res Chem Intermed 41:169–174
38. Huang L, Lei T, Lin C, Kuang X, Chen H, Zhou H (2010) Blumeaxanthene II, a novel xanthene from Blumea riparia DC. Fitoterapia 81:389–392
39. Paliwal P, Jetti SR, Bhatewara A, Kadre T, Jain S (2013) DABCO catalyzed synthesis of xanthene derivatives in aqueous media. ISRN Org Chem. https://doi.org/10.1155/2013/526173
40. Shabir G, Saeed A, Ali Channar P (2018) A review on the recent trends in synthetic strategies and applications of xanthene dyes. Mini Rev Org Chem 15:166–197
41. Pradeep P, Rao JS, Shubha J (2012) DABCO promoted multicomponent one-pot synthesis of xanthene derivatives. Res J Chem Sci 2:21–25
42. Poupelin J, Saint-Ruf G, Foussard-Blanpin O, Narcisse G, Uchida-Ernouf G, Lacroix R (1978) Synthesis and antiinflammatory properties of bis (2-hydroxy-1-naphthyl) methane derivatives. I. Monosubstituted derivatives. Eur J Med Chem 13:67–71
43. Singh H, Nand B, Sindhu J, Khurana JM, Sharma C, Aneja KR (2014) Efficient one pot synthesis of xanthene-triazole-quinoline/phenyl conjugates and evaluation of their antimicrobial activity. J Braz Chem Soc 25:1178–1193
44. Ilangovan A, Anandhan K, Prasad KM, Vijayakumar P, Renganathan R, Ananth DA, Sivasudha T (2015) Synthesis, DNA-binding study, and antioxidant activity of 14-aryl-14*H*-dibenzo[*a,j*]xanthene derivatives. Med Chem Res 24:344–355
45. Galt RHB, Horbury J, Matusiak ZS, Pearce RJ, Shaw JS (1989) The xanthene-9-spiro-4′-piperidine nucleus as a probe for opiate activity. J Med Chem 32:2357–2362
46. Spatafora C, Barresi V, Bhusainahalli VM, Di Micco S, Musso N, Riccio R, Bifulco G, Condorelli D, Tringali C (2014) Bio-inspired benzo[*k,l*]xanthene lignans: synthesis, DNA-interaction and antiproliferative properties. Org Biomol Chem 12:2686–2701
47. Rahmati A (2010) A rapid and efficient method for the synthesis of 14*H*-dibenzo[α.*j*]xanthenes, aryl-5*H*-dibenzo[*bi*]xanthene-5,7,12,14-(13*H*)-tetraone and 1,8-dioxo-octahydroxanthenes by acidic ionic liquid. Chin Chem Lett 21:761–764
48. Hideo T, Teruomi J (1981) Benzopyrano[2,3-*b*]xanthene derivatives. Jpn Tokkyo Koho JP 56005480:80922b
49. Banerjee A, Mukherjee AK (1981) Chemical aspects of santalin as a histological stain. Stain Technol 56:83–85
50. Singh H, Sindhu J, Khurana JM (2015) Synthesis of novel fluorescence xanthene–aminoquinoline conjugates, determination of dipole moment and selective fluorescence chemosensor for Th^{4+} ions. Opt Mater (Amst) 42:449–457
51. Katori A, Azuma E, Ishimura H, Kuramochi K, Tsubaki K (2015) Fluorescent dyes with directly connected xanthone and xanthene units. J Org Chem 80:4603–4610
52. Belov VN, Mitronova GY, Bossi ML, Boyarskiy VP, Hebisch E, Geisler C, Kolmakov K, Wurm CA, Willig KI, Hell SW (2014) Masked rhodamine dyes of five principal colors revealed by photolysis of a 2-diazo-1-indanone caging group: synthesis, photophysics, and light microscopy applications. Chem Eur J 20:13162–13173
53. Shaterian HR, Sedghipour M, Mollashahi E (2014) Brønsted acidic ionic liquids catalyzed the preparation of 13-aryl-5*H*-dibenzo[*b,i*]xanthene-5,7,12,14(13*H*)-tetraones and 3,4-dihydro-1*H*-benzo[*b*]xanthene-1,6,11(2*H*,12*H*)-triones. Res Chem Intermed 40:1345–1355
54. Khurana JM, Lumb A, Chaudhary A, Nand B (2014) Acid catalyzed efficient syntheses of aryl-5*H*-dibenzo[*b,i*]xanthene-5,7,12,14-(13*H*)-tetraones and 3,3-(arylmethylene) bis (2-hydroxynaphthalene-1,4-diones) and in vitro evaluation of their antioxidant activity. J Heterocycl Chem 51:1747–1751
55. Liu P, Hao J-W, Liang S-J, Liang G-L, Wang J-Y, Zhang Z-H (2016) Choline chloride and itaconic acid-based deep eutectic solvent as an efficient and reusable medium for the preparation of 13-aryl-5*H*-dibenzo[*b,i*]xanthene-5,7,12,14(13*H*)-tetraones. Monatsh Chem 147:801–808
56. Casiraghi G, Casnati G, Catellani M, Corina M (1974) A convenient one-step synthesis of xanthene derivatives. Synthesis (Stuttg) 1974:564
57. Seyyedhamzeh M, Mirzaei P, Bazgir A (2008) Solvent-free synthesis of aryl-14*H*-dibenzo[*a,j*]xanthenes and 1,8-dioxo-octahydro-xanthenes using silica sulfuric acid as catalyst. Dye Pigment 76:836–839
58. Bazgir A, Tisseh ZN, Mirzaei P (2008) An efficient synthesis of spiro[dibenzo[*b,i*]xanthene-13,3′-indoline]-pentaones and 5*H*-dibenzo[*b,i*]xanthene-tetraones. Tetrahedron Lett 49:5165–5168
59. Heravi MM, Alinejhad H, Bakhtiari K, Saeedi M, Oskooie HA, Bamoharram FF (2011) Solvent-free synthesis of xanthene derivatives by preyssler type heteropolyacid. Bull Chem Soc Ethiop 25:399–406
60. Ilangovan A, Malayappasamy S, Muralidharan S, Maruthamuthu S (2011) A highly efficient green synthesis of 1,8-dioxo-octahydroxanthenes. Chem Cent J 5:81
61. Kaya M (2011) Aldol condensation and Michael addition of 4,4-dimethyl-cyclohexane-1,3-dione and aromatic aldehydes. Unconventional substituent effects. Chin J Chem 29:2355–2360
62. Maghsoodlou MT, Khorshidi N, Mousavi MR, Hazeri N, Habibi-Khorassani SM (2015) Starch solution as an efficient and environment-friendly catalyst for one-pot synthesis of β-aminoketones and 2,3-dihydroquinazolin-4(1*H*)-ones in EtOH. Res Chem Intermed 41:7497–7508
63. Mousavi SR (2016) Claisen–Schmidt condensation: synthesis of (1S,6R)/(1R,6S)-2-oxo-*N*,4,6-triarylcyclohex-3-enecarboxamide derivatives with different substituents in H_2O/EtOH. Chirality 28:728–736
64. Mousavi MR, Gharari H, Maghsoodlou MT, Hazeri N (2016) Acetic acid-promoted eco-friendly one-pot pseudo six-component synthesis of bis-spiro-substituted piperidines. Res Chem Intermed 42:3875–3886
65. Mousavi SR, Sereshti H, Rashidi Nodeh H, Foroumadi A (2019) A novel and reusable magnetic nanocatalyst developed based on graphene oxide incorporated strontium nanoparticles for the facial synthesis of β-enamino ketones under solvent-free conditions. Appl Organomet Chem 33:e4644
66. Ilangovan A, Muralidharan S, Sakthivel P, Malayappasamy S, Karuppusamy S, Kaushik MP (2013) Simple and cost effective acid catalysts for efficient synthesis of 9-aryl-1,8-dioxooctahydroxanthene. Tetrahedron Lett 54:491–494
67. Venkatesan K, Pujari SS, Lahoti RJ, Srinivasan KV (2008) An efficient synthesis of 1, 8-dioxo-octahydro-xanthene derivatives promoted by a room temperature ionic liquid at ambient conditions under ultrasound irradiation. Ultrason Sonochem 15:548–553
68. Kokkirala S, Sabbavarapu NM, Yadavalli VDN (2011) β-Cyclodextrin mediated synthesis of 1,8-dioxooctahydroxanthenes in water. Eur J Chem 2:272–275

69. Li J-J, Tao X-Y, Zhang Z-H (2008) An effective bismuth trichloride-catalyzed synthesis of 1,8-dioxo-octahydroxanthenes. Phosphorus, Sulfur, Silicon 183:1672–1678
70. Khaligh NG (2018) Synthesis and characterization of novel binuclear task-specific ionic liquid: an efficient and sustainable sulfonic-functionalized ionic liquid for one-pot synthesis of xanthenes. Res Chem Intermed 44:4045–4062
71. Waghmare AS, Kadam KR, Pandit SS (2011) Hypervalent iodine catalysed synthesis of 1,8-dioxooctahydroxanthenes in aqueous media. Arch Appl Sci Res 3:423–427
72. Li Y, Du B, Xu X, Shi D, Ji S (2009) A green and efficient synthesis of 13-aryl-5,7,12,14-tetrahydrodibenzo[*b,i*]xanthene-5,7,12,14(13*H*)-tetraone derivatives in ionic liquid. Chin J Chem 27:1563–1568
73. Tisseh ZN, Azimi SC, Mirzaei P, Bazgir A (2008) The efficient synthesis of aryl-5*H*-dibenzo[*b,i*]xanthene-5,7,12,14(13*H*)-tetraone leuco-dye derivatives. Dye Pigment 79:273–275
74. Khaligh NG, Shirini F (2015) *N*-Sulfonic acid poly (4-vinylpyridinium) hydrogen sulfate as an efficient and reusable solid acid catalyst for one-pot synthesis of xanthene derivatives in dry media under ultrasound irradiation. Ultrason Sonochem 22:397–403

Affiliations

Seyyed Rasul Mousavi[1] · Hamid Rashidi Nodeh[2] · Elham Zamiri Afshari[3] · Alireza Foroumadi[1]

✉ Alireza Foroumadi
aforoumadi@yahoo.com

[1] Department of Medicinal Chemistry, Faculty of Pharmacy and The Institute of Pharmaceutical Sciences (TIPS), Tehran University of Medical Sciences, Tehran, Iran

[2] Department of Food science & Technology, Faculty of Food Industry and Agriculture, Standard Research Institute (SRI), P.O. Box: 31745-139, Karaj, Iran

[3] Department of Chemistry, Faculty of Science, University of Tehran, Tehran, Iran